The American Journal of Human Genetics, Volume *105*

Supplemental Data

RPL13 Variants Cause Spondyloepimetaphyseal Dysplasia with Severe Short Stature

Cedric Le Caignec, Benjamin Ory, François Lamoureux, Marie-Francoise O'Donohue, Emilien Orgebin, Pierre Lindenbaum, Stéphane Téletchéa, Manon Saby, Anna Hurst, Katherine Nelson, Shawn R. Gilbert, Yael Wilnai, Leonid Zeitlin, Eitan Segev, Robel Tesfaye, Mathilde Nizon, Benjamin Cogne, Stéphane Bezieau, Loic Geoffroy, Antoine Hamel, Emmanuelle Mayrargue, Benoît de Courtivron, Aliette Decock-Giraudaud, Céline Charrier, Olivier Pichon, Christelle Retière, Richard Redon, Alexander Pepler, Kirsty McWalter, Lydie Da Costa, Annick Toutain, Pierre-Emmanuel Gleizes, Marc Baud'huin, and Bertrand Isidor

Figure S1

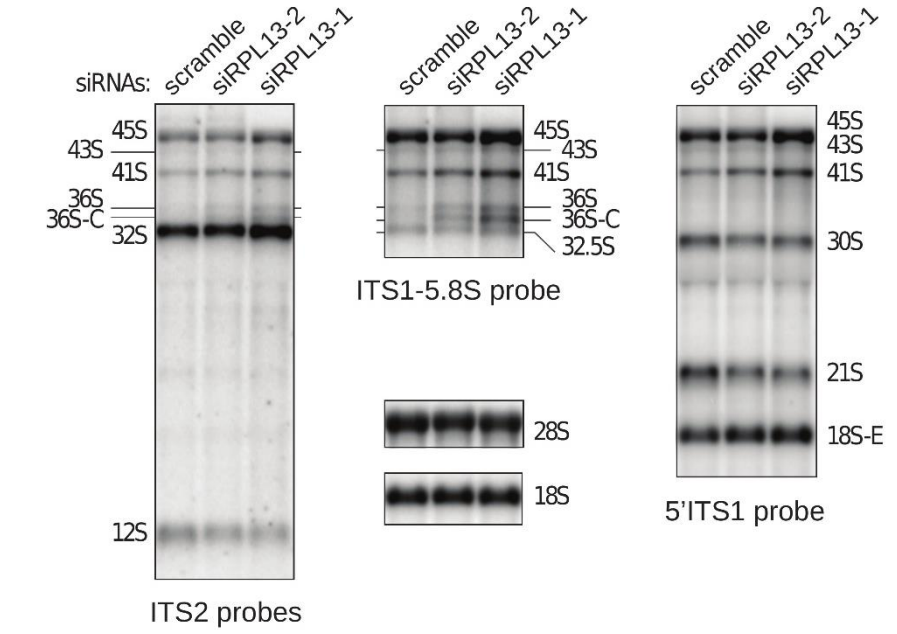
siRNAs:
scramble
siRPL13-2
siRPL13-1
45S
43S
41S
36S
36S-C
32S
12S
ITS2 probes
32.5S
ITS1-5.8S probe
28S
18S
30S
21S
18S-E
5'ITS1 probe

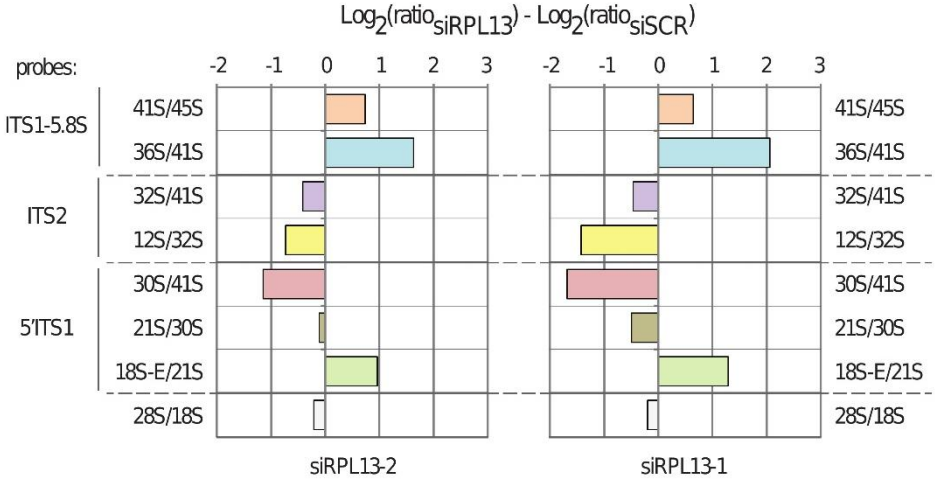
Log2(ratio siRPL13) - Log2(ratio siSCR)
probes:
-2
-1
0
1
2
3
ITS1-5.8S
ITS2
5'ITS1
41S/45S
36S/41S
32S/41S
12S/32S
30S/41S
21S/30S
18S-E/21S
28S/18S
siRPL13-2
siRPL13-1

Figure S2

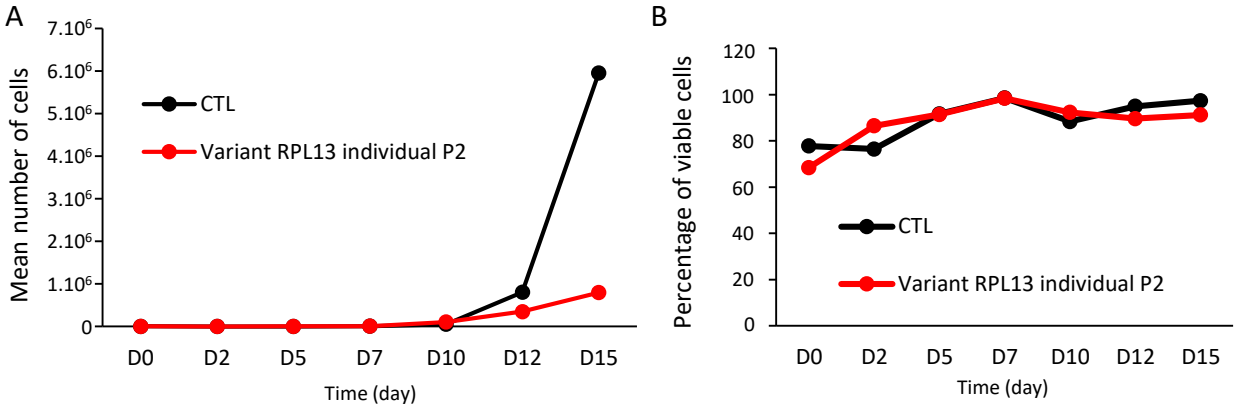
A
Mean number of cells
7.10⁶
6.10⁶
5.10⁶
4.10⁶
3.10⁶
2.10⁶
1.10⁶
0
CTL
Variant RPL13 individual P2
D0
D2
D5
D7
D10
D12
D15
Time (day)
B
Percentage of viable cells
120
100
80
60
40
20
0
CTL
Variant RPL13 individual P2
D0
D2
D5
D7
D10
D12
D15
Time (day)

SUPPLEMENTAL FIGURE LEGENDS

Figure S1. Consequence of mutant RPL13 on pre-rRNA processing.

Northern blot analysis of pre-RNAs in lymphoblastoid cells treated with siRNAs targeting RPL13 mRNAs. The 5'ITS1 and the ITS2 probes detect the precursors to the 40S and 60S subunit RNAs, respectively. The ITS1-5.8S probe evidences an accumulation of 36S and 36S-C precursors when the level of RPL13 is reduced, which is indicative of a defect in cleavage at site 2. This cleavage occurs early and produces two separate pathways for the small and large ribosomal precursors.

Figure S2 : Erythroid proliferation is decreased in the variant RPL13 individual compared to the healthy control.

(A) Mean erythroid progenitor cell proliferation and (B) cell viability of peripheral $CD34^{+}$ cells from the variant RPL13 individual and from the control, from D0 to D15 during the complete erythroid differentiation (Mean of technical triplicates).

Table S1 : Primers for RPL13 RT-PCR

	Forward	Reverse
RPL13 (NM_000977.3)	ATGGCGCCCAGCCGGAATGG	AAACACACCACGTGGAGACC

MATERIALS AND METHODS

Individuals and Exome sequencing

Exome sequencing was performed in individuals P1, P2 and their parents following previously described procedures[1]. Through GeneMatcher[2], we subsequently identified two additional individuals (P3 and P4), yielding a total of four affected subjects from four families. All variants were confirmed by Sanger sequencing. We obtained written informed consent from all study participants in accordance with a protocol approved by respective institutional review boards (Nantes CHU ethical committee (MESR DC-2017-2987))

Fastqs of 60 samples (P1, P2, their parents and 54 samples unrelated to the present study) were mapped to grch37 using bwa-mem 0.7.12 and called with GATK 3.7.0 according to the Broad-Institute best-practices but the variants were not recalibrated because there were not enough data. The resulting VCF was annotated with SnpEff 4.3 and the gnomad database. De-novo genotypes called in either P1 and P2 but absent for the other individuals, missing in gnomad, were selected using vcffilterjs and grouped by gene using jvarkit/groupbygene. The candidate variants were visually checked with IGV.

The coding regions and flanking intronic regions of individual P3 and its parents were enriched using Agilent SureSelect XT All Exon V7 in-solution technology and were sequenced using the Illumina NovaSeq system. Illumina bcl2fastq2 was used to demultiplex sequencing reads. The reads were mapped to the human reference genome (hg19) using the Burrows Wheeler Aligner, and variants were called using Samtools and Varscan. Variants in the coding region and the flanking intronic regions (±8 bp) with a minor allele frequency (MAF) < 1.5% were evaluated. Known disease-causing variants (according to HGMD) within ±30 bp of flanking regions and up to 5% MAF were also evaluated. MAFs were taken from gnomAD and an in-house database. NGS based CNV calling was computed using an internally-developed method based on sequencing coverage depth; a model of the expected coverage that represents wet-lab biases as

well as inter-sample variation was used. CNV calling was performed by computing the sample's normalized coverage profile and its deviation from the expected coverage. Variants found in patient P3 and in its parents were compared and filtered for four cases: *de novo* in the patient, patient is compound heterozygous, patient is homozygous and the parents are heterozygous, patient is hemizygous and the mother is heterozygous for variants on the X-chromosome. Variants were evaluated based on the ACMG guidelines for the interpretation of sequence variants. Several additional in-silico panels were used to exclude the possible presence of non-trio variants which could explain the phenotype of the patient.

Using genomic DNA from individual P4 and parents, the exonic regions and flanking splice junctions of the genome were captured using the IDT xGen Exome Research Panel v1.0. Massively parallel (NextGen) sequencing was done on an Illumina system with 100bp or greater paired-end reads. Reads were aligned to human genome build GRCh37/UCSC hg19, and analyzed for sequence variants using a custom-developed analysis tool. Additional sequencing technology and variant interpretation protocol has been previously described [3]. The general assertion criteria for variant classification are publicly available on the GeneDx ClinVar submission page http://www.ncbi.nlm.nih.gov/clinvar/submitters/26957/

Reverse transcription–PCR.

Total RNA was extracted from peripheral blood cells (P1 and P2), using TriReagent (Life Technologies). Total RNA was reversed transcribed using the ThermoScript RT–PCR System (Life Technologies). Two microliters of the RT reaction were subjected to Polymerase Chain Reaction (Life Technologies) using 0.2 µM of forward and reverse primers (Table S1). PCR were carried for 30 cycles. Each cycle consisted of 1 minute of denaturation at 94°C, 1 minute of annealing at 62°C and 1 minute of extension at 72°C. PCR products were were separated in a 1,7% agarose/1x TAE gel at 120 V for 1 hour and stained with SybrSafe (Life Technologies).

Pictures of the gel were taken by CCD camera under UV light (Syngene) and are representative of 3 independent experiments.

Western blotting analysis

Lymphoblastoid cells were established by EBV transformation of peripheral B cells using EBV supernatant harvested from the cell line B95-8 (American Type Culture Collection). Mesenchymal stem cells (P1 and healthy donor) and lymphoblastoid cells (P2 and healthy donor) were cultured respectively α-MEM and RPMI (GIBCO). Healthy donor cells were not matched for age and sex with individuals P1 and P2 cells. After cells lysis, samples containing equal amounts of protein (50 µg) were separated on 16% SDS-polyacrylamide gels, and proteins were transferred to polyvinylidene difluoride membranes. The membranes were blocked in blocking buffer (LiCor, USA) at room temperature for 1 hour and blots were probed overnight at 4 °C with primary antibodies (RPL13, 1:800; Sigma-Aldrich) or vinculin (1:10.000; Cell signaling) to detect proteins of interests. After incubation, the membranes were washed three times with washing buffer (PBS containing 0.1% Tween) for 5 minutes. Membranes were then incubated for 1 hour with 1:10,000 diluted secondary antibodies (Li-Cor) at room temperature. Specific proteins were detected using Odyssey Fc (Li-Cor) after washing. Pictures are representative of 3 independent experiments.

Structural modelling

The protein structure of the mutated RPL13 protein was predicted using I-TASSER 5.1 [4-6]. I-TASSER selected the structure of the human ribosome as the best template (4V6X, [7]) to build high quality models. Visual inspection of models and interaction analysis were done with PyMOL 1.8 [8].

Tissue culture and siRNA treatment

HeLa cells were cultured in DMEM (GIBCO) supplemented with 10% fetal bovine serum and 1 mM sodium pyruvate (Sigma). Two 21-mer siRNA duplexes (Eurogentec) were used to knock down expression of the human RPL13 mRNAs in HeLa cells (siRPL13-1: 5'-GGAAGAGAAGAAUUUCAAAdTdT-3'; siRPL13-2: 5'-CGUCUAUAAGAAGGAGAAAdTdT-3'). Knockdown efficiency was verified by qPCR. Each siRNA solution was added at a final concentration of 500 nM to 200 ml of cell suspension (50.10^6 cells/ml diluted in Na phosphate buffer, pH 7.25, containing 250 mM sucrose and 1 mM MgCl2). Electro-transformation was performed at 240 V with a Gene Pulser (Bio-Rad)[9]. Control HeLa cells were electro-transformed with a scramble siRNA (siRNA-negative control duplex; Eurogentec). After 10 minutes of incubation at ambient temperature, cells were plated and grown at 37°C for 48 hours.

RNA extraction and analysis by northern blot

Total RNAs were extracted with TriReagent from cell pellets containing $20\text{-}30.10^6$ cells. The aqueous phase was further extracted with phenol-chloroform-isoamylic alcohol (25:24:1; Sigma), then with chloroform. Total RNAs were recovered after precipitation with 2-propanol. For Northern blot analyses, RNAs were dissolved in formamide, denatured for 10 minutes at 70°C, and separated on a 1.2% agarose gel containing 1.2% formaldehyde and 1X Tri/Tri buffer (30 mM triethanolamine, 30 mM tricine, pH 7.9) (3 µg RNAs/lane). RNAs were transferred to a Hybond N^+ nylon membrane (GE Healthcare) by passive transfer and cross-linked under UV light. Pre-hybridization was performed for 1 hour at 45°C in 6X SSC, 5X Denhardt's solution, 0.5% SDS, 0.9 g/ml tRNA. The 5'-radiolabeled oligonucleotide probe was incubated overnight. The sequences of the probes were: 5'-ITS1 (50-CCTCGCCCTCCGGGCTCCGTTAATGATC-

3'), ITS1-5.8S (5'-CTAAGAGTCGTACGAGGTCG-3'), ITS2 (ITS2b: 5'-CTGCGAGGGAACCCCCAGCCGCGCA-3' and ITS2d/e: 5'-GCGCGACGGCGGACGACACCGCGGCGTC-3'), 18S (5'-TTTACTTCCTCTAGATAGTCAAGTTCGACC-3'), 28S (5'-CCCGTTCCCTTGGCTGTGGTTTCGCTAGATA-3'). Membranes were washed twice for 10 minutes in 2X SSC, 0.1% SDS and once in 1X SSC, 0.1% SDS, and then exposed. Signals were acquired with a Typhoon Trio PhosphorImager (GE Healthcare) and quantified using the MultiGauge software. Pictures are representative of 3 independent experiments.

Polysome profiling

Lymphoblastoid cells (healthy donors and individual 2) were treated with 100 µg/ml cycloheximide (Sigma-Aldrich) for 10 min. The cytoplasmic fractions were prepared on ice as described above, except that cycloheximide was added to all buffers [10]. A sample volume containing 1 mg of total proteins was loaded on a 10–50% (wt/wt) sucrose gradient and the tubes were centrifuged at 36 000 rpm and at 4°C for 2 hours in a SW41 rotor (Optima L100XP ultracentrifuge; Beckman Coulter). The gradient fractions were collected at OD254 nm with a Foxy Jr. gradient collector (Teledyne Isco). Each fraction was centrifuged on a Vivaspin 500 concentrator (Sartotrius Stedim Biotech) in order to remove sucrose. Half of it was then used for RNA extraction with TriReagent, while the other half was used to extract total proteins with TCA.

Culture of human primary cells

CD34+ cells from peripheral blood of individual P2 and a healthy control were isolated by immunomagnetic technique using manual column (Miltenyi Biotec, Paris, France). Purified CD34+ cells were cultured in IMDM medium using 3% AB serum (Sigma Aldrich), 2% human peripheral blood plasma (stem cell technologies), 10 µg/ml Insulin (Sigma Aldrich), 3U/ml

Heparin (Sigma Aldrich), 200 µg/ml Holo-Transferrin (Sigma Aldrich), 10 ng/ml stem cell factor (SCF) (Miltenyl biotech), 1 ng/ml IL3 (Stem Cell Technologies), 3 IU/ml EPO and 1% Penicillin/Streptomycin (final concentrations). This media was used from day 0 to day 6, then deprivated from IL3 and EPO concentration was used at 1 IU/ml from day 7 to day 10. From day 11 to day 15, SCF was removed and EPO and Holo-Transferrin was used respectively at 0.1 IU/ml and 1 mg/ml, and 100% Penicillin/Streptomycin (final concentrations). Viable cells were counted in triplicate using the trypan blue dye exclusion test as a function of time in culture. Bars represent mean of technical triplicate.

Immunochemistry

All procedures involving mice (their housing and care in the Experimental Therapeutic Unit at the Faculty of Medicine of Nantes, France, the method by which they were anesthetized and killed, and all experimental protocols) were conducted in accordance with the institutional guidelines of the French Ethical Committee (CEEA.PdL.2011.32). Eight-week old C57BL/6 male mice were sacrificed, tibiae were collected and were decalcified with 4.13% EDTA and 0.2% paraformaldehyde in phosphate buffered saline (PBS) for 96 hours using the KOS microwave histostation (Milestone, Kalamazoo, MI) before embedding in paraffin. Sections (3 µm thick, Leica Microsystems) were analyzed by immunostaining for RPL13, RPL3, RPS3 and RPS10. Protocols were performed as described previously [11] with rabbit anti-RPL13, anti-RPL3, anti-RPS3 and anti-RPS10 antibodies (1/800; Sigma for RPL13 and 1/1000 GeneTex for RPL3, RPS3 and RPS10).

REFERENCES OF SUPPLEMENTAL DATA

1. Isidor, B., Lindenbaum, P., Pichon, O., Bezieau, S., Dina, C., Jacquemont, S., Martin-Coignard, D., Thauvin-Robinet, C., Le Merrer, M., Mandel, J.L., et al. (2011). Truncating mutations in the last exon of NOTCH2 cause a rare skeletal disorder with osteoporosis. Nature genetics 43, 306-308.
2. Sobreira, N., Schiettecatte, F., Valle, D., and Hamosh, A. (2015). GeneMatcher: a matching tool for connecting investigators with an interest in the same gene. Hum Mutat 36, 928-930.
3. Retterer, K., Juusola, J., Cho, M.T., Vitazka, P., Millan, F., Gibellini, F., Vertino-Bell, A., Smaoui, N., Neidich, J., Monaghan, K.G., et al. (2016). Clinical application of whole-exome sequencing across clinical indications. Genet Med 18, 696-704.
4. Roy, A., Kucukural, A., and Zhang, Y. (2010). I-TASSER: a unified platform for automated protein structure and function prediction. Nature protocols 5, 725-738.
5. Yang, J., Yan, R., Roy, A., Xu, D., Poisson, J., and Zhang, Y. (2015). The I-TASSER Suite: protein structure and function prediction. Nature methods 12, 7-8.
6. Zhang, Y. (2008). I-TASSER server for protein 3D structure prediction. BMC bioinformatics 9, 40.
7. Anger, A.M., Armache, J.P., Berninghausen, O., Habeck, M., Subklewe, M., Wilson, D.N., and Beckmann, R. (2013). Structures of the human and Drosophila 80S ribosome. Nature 497, 80-85.
8. Schrödinger, L. (2015). The PyMOL Molecular Graphics System, Version 1.8.
9. Paganin-Gioanni, A., Bellard, E., Escoffre, J.M., Rols, M.P., Teissie, J., and Golzio, M. (2011). Direct visualization at the single-cell level of siRNA electrotransfer into cancer cells. Proceedings of the National Academy of Sciences of the United States of America 108, 10443-10447.
10. Baudin-Baillieu, A., Hatin, I., Legendre, R., and Namy, O. (2016). Translation Analysis at the Genome Scale by Ribosome Profiling. Methods Mol Biol 1361, 105-124.
11. Baud'huin, M., Lamoureux, F., Jacques, C., Rodriguez Calleja, L., Quillard, T., Charrier, C., Amiaud, J., Berreur, M., Brounais-LeRoyer, B., Owen, R., et al. (2017). Inhibition of BET proteins and epigenetic signaling as a potential treatment for osteoporosis. Bone 94, 10-21.